



**HAL**  
open science

## Spreading and absorption of a drop on a swelling surface

Pierre van de Velde, Nathalie Fabre-Parras, Christophe Josserand, Camille Duprat, Suzie Protière

► **To cite this version:**

Pierre van de Velde, Nathalie Fabre-Parras, Christophe Josserand, Camille Duprat, Suzie Protière. Spreading and absorption of a drop on a swelling surface. *EPL - Europhysics Letters*, 2023, 144 (3), pp.33001. 10.1209/0295-5075/ad0eed . hal-04424485

**HAL Id: hal-04424485**


**<https://hal.science/hal-04424485>**

Submitted on 29 Jan 2024

**HAL** is a multi-disciplinary open access archive for the deposit and dissemination of scientific research documents, whether they are published or not. The documents may come from teaching and research institutions in France or abroad, or from public or private research centers.

L'archive ouverte pluridisciplinaire **HAL**, est destinée au dépôt et à la diffusion de documents scientifiques de niveau recherche, publiés ou non, émanant des établissements d'enseignement et de recherche français ou étrangers, des laboratoires publics ou privés.

# Spreading and absorption of a drop on a swelling surface

PIERRE VAN DE VELDE<sup>1(a)</sup> , NATHALIE FABRE-PARRAS<sup>1</sup>, CHRISTOPHE JOSSE-  
RAND<sup>1</sup>, CAMILLE DUPRAT<sup>1</sup>  
and SUZIE PROTIÈRE<sup>2</sup>

<sup>1</sup> *LadHyX, Ecole Polytechnique, UMR 7646 - F-91128 Palaiseau Cedex, France*

<sup>2</sup> *Institut Jean le Rond d'Alembert, Sorbonne Université, CNRS, UMR 7190 - F-75005, Paris, France*

**Abstract** – When a drop is placed on a surface it fully wets, it usually spreads until the height of the drop is comparable to the size of a single fluid molecule. However, when some fluid is absorbed by the substrate, the drop will first spread to a given radius before receding and eventually disappearing completely. In this study, we consider the spreading and absorption of a silicone oil drop on a swelling elastomeric substrate. We observe that the maximal radius of the drop does not depend on the fluid viscosity and can be predicted from the droplet volume and material properties. We rationalize our observations with a scaling analysis and a model coupling the spreading to a linear poroelastic description of the elastomer.

**Introduction.** – The canonical case of a drop spreading on an ideal flat and fully wetting surface has been extensively examined in the past, leading to various scalings for the radius in time [1–8]. Depending on the conditions, the spreading dynamics are dominated by inertial, viscous, or gravitational effects. In principle, the drop spreads until its height becomes comparable to the molecular size. However, in most real systems, the substrate is not an ideally flat and inert surface and the spreading is affected by its roughness, deformations, chemical interactions or by its absorption of fluid. On rough surfaces, such as a paper sheet or wood, the spreading of the drop may be prevented due to pinning of the contact line [6,9]. When placed on a liquid film containing surfactants, the spreading of the drop may even be followed by a recoiling phenomenon [10]. On very elastic substrates, such as hydrogels [11,12] or soft elastomers [13], the local deformation of the surface can pin the contact line or slow down the spreading. Free chains in the elastomer may even be affected by these deformations and induce further dissipations. Liquids spreading on absorbing substrates are common to a variety of systems such as inkjet printers [9], face masks [14] or drops impacting porous walls [15] for example. How far a drop spreads and how long it takes for the liquid to penetrate the substrate are naturally arising questions when it can absorb the liquid. In this work, we will consider the effect of an absorbing, swelling substrate on the spreading of a drop. The

drop volume is hence no longer constant which leads to a decrease of the drop radius. Studies on idealized porous surfaces have examined the coupled spreading and absorption problem both theoretically [16–19], numerically [16] and experimentally [6]. In the particular case of swellable substrates, the absorption of the drop leads to a local and transient deformation of the solid. Several experimental studies have described the absorption of solvent drops on flat elastomeric surfaces, describing the resulting macroscopic deformations [20] or the appearance of creases at the polymer surface [21]. Other works have described the absorption of water drops into thin hydrogel slabs [12] or the absorption of droplet trains impacting an elastomeric cylinder [22]. In most studies describing the absorption of drops on swelling substrates, the drop is pinned and has a non-zero contact angle. To the best of our knowledge, a study of the coupled spreading and absorption problem in the case of a fully wetting fluid on a swellable substrate is still lacking. In this letter, we observe the spreading dynamics of a drop placed on an initially flat but swellable elastomeric surface. The equilibrium contact angle is close to zero and the contact line is free to move throughout the experiment. The drop first spreads before retracting as it is absorbed by the elastomer. We find that the maximal radius of the drop is independent of the fluid viscosity and rationalize this observation by a scaling analysis. We then develop a model coupling the spreading of the drop to a linear poroelastic theory describing the absorption of the fluid into the polymeric network, capturing the main

<sup>(a)</sup>E-mail: pierre.van.de.velde@ulb.be (corresponding author)

physical ingredients of the problem and accurately predicting the maximal spreading radius.

### Spreading and retraction of a drop on a flat substrate.

– We fabricate flat elastomeric substrates out of either polyvinylsiloxane (PVS, Zhermack Elite Double 8,  $E = 0.2$  MPa or 32,  $E = 0.9$  MPa) or polydimethylsiloxane (PDMS, Corning,  $E = 1$  MPa). Both are silicone-based elastomers that swell in contact with a low-viscosity silicone oil. We combine the liquid elastomer with a catalyst before pouring the obtained solution into cylindrical molds and degassing to avoid the presence of air bubbles in the final polymer. After reticulation, the polymeric cylinders (of diameter 2.3 cm) are pulled out of the wells. No chemical treatment is done to the molds. To realize the experiments, a polymeric cylinder is placed onto a small support ensuring its upper surface is perpendicular to gravity. We then carefully place a drop of fully wetting liquid silicone oil (Carl Roth, viscosity  $\eta = 2.3$ – $10.5$  mPa  $\cdot$  s, surface tension  $\gamma = 0.018$  N  $\cdot$  m $^{-1}$ ) on the surface with zero initial velocity using a needle connected to a syringe pump (Aladdin, SyringeONE). To measure the deposited volume of oil precisely, the polymer blocks are weighed using a precision balance (Mettler Toledo, 0.00001 g precision) before and after the experiment. We track the evolution of the drops during their spreading and absorption using a digital camera (Nikon D810) with a 105 mm macro lens taking an image every two seconds.

Typical images for a drop of 4  $\mu$ l are presented in fig. 1. The drop fully wets the substrate, and initially spreads quickly, forming a relatively flat drop (fig. 1(a)). After several seconds, the spreading slows down until the drop reaches its maximal radius  $R_{max}$  at  $t = 12$  s (fig. 1(b)). The drop then retracts until it is completely absorbed by the PVS (fig. 1(c)). The final result is a small bump at the surface of the PVS (fig. 1(d)) which relaxes within a few hours by diffusion of the oil within the block. To enhance the contrast and to track the drop radius precisely, we place an obstacle, such as an opaque sheet of paper in the light path between the led panel shown on the drop. As is the case for a dark field microscope, only light that is deflected or reflected by the drop will appear on the images. Figures 2(A) and (B) show typical images during the drop spreading and receding. To get the evolution of  $R$  in time, we perform a reslice along the long axis of the drop using ImageJ and obtain an image showing the edge of the drop during spreading and retraction, giving readily  $R(t)$ . Figure 3 presents measurements of  $R(t)$  obtained for different oil viscosities and drop volumes. The error bars correspond to measurement errors during the image post-processing. During the retraction phase in particular, the edge of the drop becomes difficult to track as it becomes irregular and less sharp on the images (fig. 2(B)). Nonetheless, we can get a good estimation of  $R(t)$  as the wet parts of the polymer appear darker than their surrounding dry parts. Controlling the exact

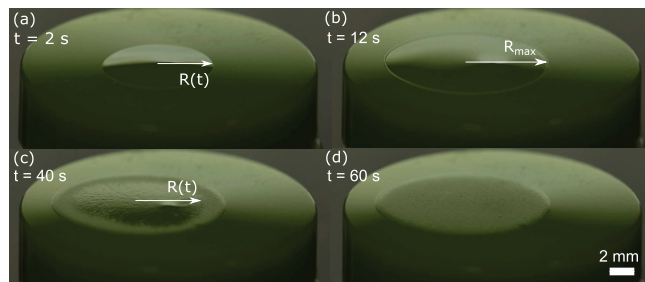


Fig. 1: Spreading of a drop. A drop of low-viscosity silicone oil ( $\eta = 2.3$  mPa  $\cdot$  s,  $V = 4$   $\mu$ l) is deposited onto a flat PVS substrate. The drop spreads rapidly until it reaches its maximal radius  $R_{max}$  at  $t = 12$  s. From there, it retracts as it is progressively absorbed by the PVS substrate.

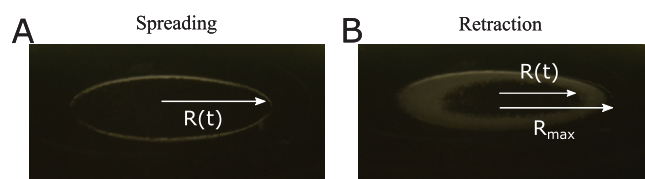


Fig. 2: Measuring the drop radius. Pictures used to measure the drop radius during spreading and retraction. To enhance the contrast, an obstacle is placed between the drop and the backlight to show only light that is deflected by the drops.

deposited value is also difficult as some fluid remains on the needle tip after deposition. For comparable volumes ( $\Delta V < 0.1$   $\mu$ l), the differences in  $R(t)$  are of the same order as the measurement error (about  $\pm 1$  mm). For all experiments, the drop radius first sharply increases up to an inflection point where the slope of  $R(t)$  decreases slowly until it finally reaches a maximum value  $R_{max}$  at a time we call  $\tau_{max}$ . From there, the absorption of the drop dominates the spreading, and  $R(t)$  begins to decrease until the drop is fully absorbed at  $t = \tau_f$ .  $\tau_f$  increases both with drop volume and viscosity, which is intuitive as both the spreading and the absorption are slower for more viscous fluids. Figure 4(A) shows the value of  $R_{max}$  depending on the volume for the three considered viscosities. Interestingly, the scattering of the data points shows that  $R_{max}$  does not depend on the liquid viscosity. However  $R_{max}$  increases with  $V$  and its exact dependence remains to be understood. In the next section, we attempt to estimate the value of  $R_{max}$  using a scaling analysis.

**Scaling analysis for  $R_{max}$ .** – To explain the independence of  $R_{max}$  on the viscosity, we construct two characteristic time scales. Generally, the spreading of a drop is driven by capillary forces as well as external forces, such as gravity. During the spreading, energy is dissipated either through viscous effects located mainly in the corner of the drop [5], or through molecular dissipation at the triple line [7]. Generally, the spreading of a drop is well captured by a power-law scaling such that  $R \sim t^\beta$  where  $\beta$  ranges from  $\frac{1}{8}$  to  $\frac{1}{10}$ . At very short times, inertia is competing against the capillary forces, leading to  $\beta = \frac{1}{2}$  [1,2]. This

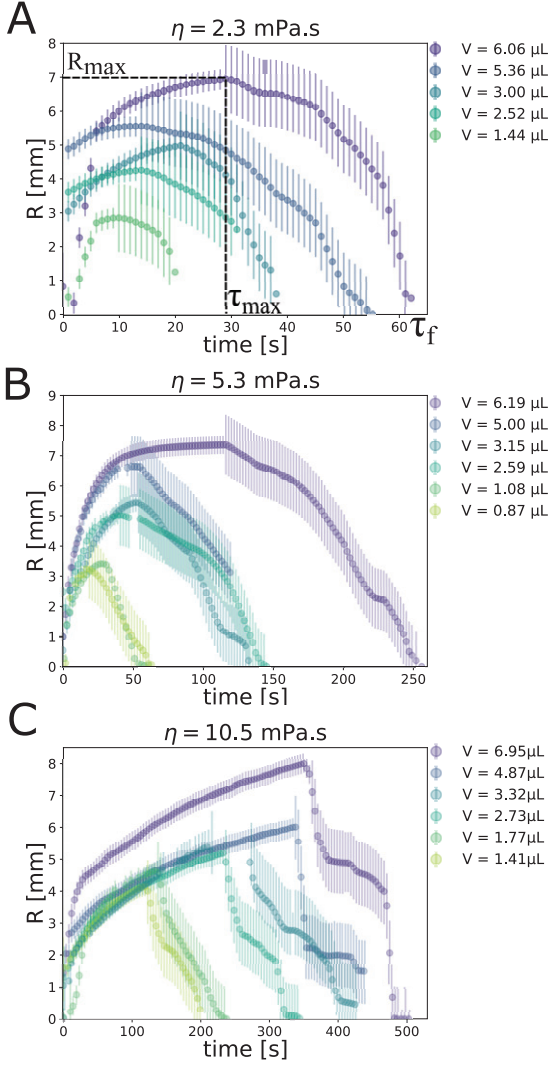


Fig. 3: Measured drop radius in time. Radius of the drop measured for different initial drop volumes and viscosities. All experiments are performed on PVS ( $E = 0.9$  MPa) For all experiments, the drop radius starts by increasing before reaching a maximal radius  $R_{max}$  and starting to retract until it is fully absorbed. Larger drop volumes or viscosities lead to longer absorption times.

rapid inertial spreading lasts only for a few milliseconds and we do not capture it in our experiments due to the camera resolution in time. In this study we focus on later stages of the spreading, once inertial effects become negligible. Indeed after this rapid initial spreading, we capture the first image at  $t = 2$  s. The drop has already reached a significant radius and continues to spread slowly. Models combining the different theories tend to consider a second spreading regime, lasting for several seconds, based on the molecular theory giving  $\beta = \frac{1}{7}$  [8]. At longer timescales, the spreading is well captured by a hydrodynamic theory leading to  $\beta = \frac{1}{10}$  also known as Tanner's law [5]: indeed by comparing the energy gain from the wetting to the dissipated power by viscosity in the corner close to

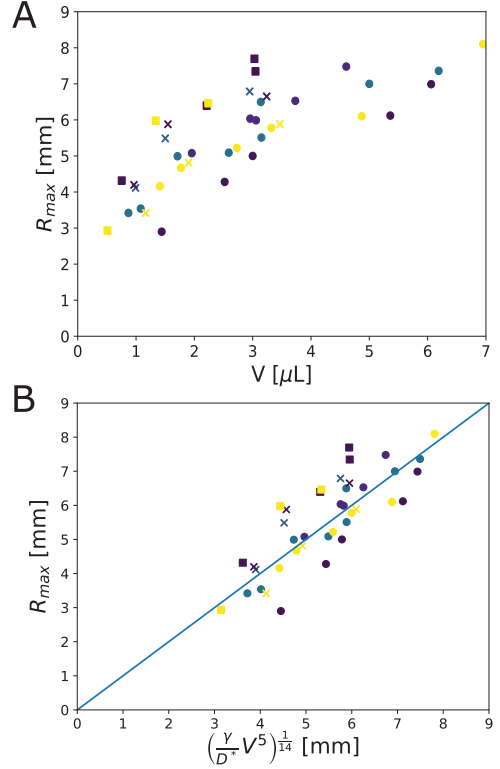


Fig. 4: Maximal drop radius. (A) Values of  $R_{max}$  obtained from our experiments on different substrate materials (x : PVS  $E = 0.2$  Mpa, o : PVS  $E = 0.9$  Mpa,  $\square$  : PDMS  $E = 1$  Mpa) and oil viscosities ( $\eta = 2.3$ , yellow; 5.4: blue; and 10.5 mPa · s: purple).  $R_{max}$  seems independent on the oil viscosity. (B) Rescaled values according to eq. (6). The blue line is a guide for the eye.

the contact line, one gets

$$R^{10} \sim \frac{\gamma V^3 t}{\eta}. \quad (1)$$

As a best guess, we construct our spreading time from Tanner's law giving us a characteristic spreading time for our problem:

$$\tau_{spread} = \frac{R_{max}^{10} \eta}{\gamma V^3}. \quad (2)$$

The swelling on the other hand can be considered as a pseudo-diffusive phenomenon. We can then construct a characteristic time as

$$\tau_{swell} = \frac{L^2 \eta}{D^*}, \quad (3)$$

where  $L$  is an appropriate lengthscale and  $D^*$  is a material-dependent constant defined such that  $D = D^*/\eta$  is a diffusion coefficient. The value of  $D^*$  is estimated by measuring the swelling dynamics of immersed elastomeric fibers and fitting its value in an empirical model [23]. To construct  $L$ , we consider a cylindrical drop of volume  $V$  and radius  $R_{max}$  giving us  $L = V/(\pi R_{max}^2)$  and thus

$$\tau_{swell} = \frac{V^2 \eta}{R_{max}^4 D^*}. \quad (4)$$

By equaling our two timescales, we obtain the following scaling for  $R_{max}$ :

$$\frac{R_{max}^{10} \eta}{\gamma V^3} \sim \frac{V^2 \eta}{R_{max}^4 D^*}, \quad (5)$$

or

$$R_{max} \sim \left( \frac{\gamma}{D^*} V^5 \right)^{\frac{1}{14}}. \quad (6)$$

Figure 4(B) shows the value of  $R_{max}$  against  $\left( \frac{\gamma}{D^*} V^5 \right)^{\frac{1}{14}}$ , where all the points seem to collapse on a line fitted from the origin (blue line). The results were obtained for three different materials (PVS 8 and 32 and PDMS) having similar diffusion coefficients. The results remained consistent with our scaling but more experiments would be needed to validate the exact dependency on  $D^*$ . We can note that our scaling predicts a very weak dependence on  $D^*$  and  $\gamma$  as the value of  $\left( \frac{\gamma}{D^*} \right)^{\frac{1}{14}}$  will always be very close to 1. The maximal swelling radius thus seems to depend almost solely on the initial drop volume. The prefactor for this scaling seems to be of the order of 1 (fig. 4(B)). More data would be necessary to confirm this value. The main limitation to the experiments comes from the difficulty of depositing very large or very small droplets on the substrate in a controlled manner, which would help to further validate this scaling. However, it exhibits clearly the independence of  $R_{max}$  from the viscosity and gives us confidence in the chosen mechanisms at play.

In the next section, we develop a model combining Tanner's law for the spreading with a linear poroelastic model for the absorption in order to describe the evolution of the drop radius over time.

**Modeling the spreading and absorption dynamics.** – The scaling obtained in the previous section confirms the idea that the maximal radius of the drop is a result of the competition between viscous spreading and poroelastic absorption of the drop. We now wish to write the equations describing both the spreading and the absorption of the drop. This will allow us to calculate the evolution of the drop radius with time as well as the maximal drop radius. By linking the change in drop volume to the total fluid flux across the interface of the polymer, we can obtain a differential equation for the drop radius. The notations used for the model are shown in fig. 5.

*Drop spreading.* We thus consider the spreading of a drop with variable volume, that fully wets the substrate (*i.e.*, the equilibrium contact angle is 0). In all that follows  $z = 0$  is defined at the initial substrate surface. We assume the drop has the shape of a spherical cap at all times (except in a very small region close to the contact line) with an apparent contact angle  $\theta(t)$ . We thus have the relation between its volume  $V(t)$ , its radius  $R(t)$  and its apparent contact angle  $\theta(t)$  at the triple line,

$$V = \frac{\pi R^3}{3 \sin^3 \theta} (2 + \cos^3 \theta - 3 \cos \theta). \quad (7)$$

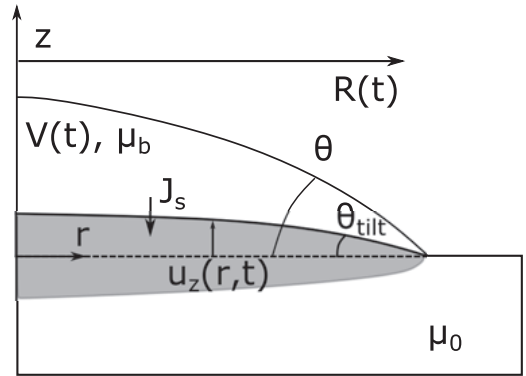


Fig. 5: Notations used to model the spreading and absorption.  $\mu_{0,b}$  denotes the chemical potential in the bulk and in the polymer (before any swelling). The grey portion represents the fluid that has penetrated the substrate. Due to the swelling, the substrate is tilted by an angle  $\theta_{tilt}$  close to the contact line.  $\theta$  is the apparent contact angle deduced by eq. (8). The surface flux is called  $J_s$ .

For small angles (*i.e.*, very thin drops), we can rewrite this as

$$R^3 = \frac{4V}{\pi \theta}. \quad (8)$$

This formula gives a relation between  $R(t)$  as a function depending on time through  $\theta(t)$  and  $V(t)$  only. Taking the time derivative of (8) one obtains

$$\frac{dR}{dt} = -\frac{1}{3} \left( \frac{4V}{\pi \theta^4} \right)^{1/3} \frac{d\theta}{dt} \Big|_V + \frac{1}{3} \left( \frac{4}{\pi V^2 \theta} \right)^{1/3} \frac{dV}{dt} \Big|_{\theta} = v_+ - v_-, \quad (9)$$

where  $\frac{d\theta}{dt} \Big|_V$  ( $\frac{dV}{dt} \Big|_{\theta}$ ) stands for the time derivative of  $\theta$  ( $V$ ) for constant  $V$  ( $\theta$ ). Inspired by the works of Starov *et al.* [18], we decompose this expression into an advancing ( $v_+ > 0$ ) and a receding ( $v_- > 0$ ) velocity contribution. In the initial steps, we consider that the dynamics is dominated by the viscous spreading. We thus calculate the advancing velocity  $v_+$  using the Tanner's law determined initially for constant volume but computed at each time using the actual drop volume  $V(t)$ . However the swelling of the material leads to an additional decrease of the contact angle in the vicinity of the contact line. To take this effect into account, we introduce the tilting angle of the substrate which is estimated as  $\theta_{tilt} = -\frac{\partial u_z}{\partial r}(R, 0, t)$ , where  $u_z(r, z, t)$  is the vertical displacement of the elastomer and thus  $u_z(r, 0, t)$  its surface displacement (see fig. 5), giving us the modified contact angle as

$$\theta = \frac{4V}{\pi R^3} + \frac{\partial u_z}{\partial r}(R, 0, t), \quad (10)$$

and thus

$$v_+ = \frac{\gamma \omega}{\eta} \left( \frac{4V}{\pi R^3} + \frac{\partial u_z}{\partial r}(R, 0, t) \right)^3, \quad (11)$$



where  $\omega$  is an apparent friction coefficient with an expression that depends on the substrate. For porous materials, as the fluid present in the material may allow slip, it is hard to estimate [24]. We thus use it as a fitting parameter in our calculations. To find  $v_-$ , we need to calculate the variation in time of the drop volume. As the liquid is absorbed by the elastomer, the drop volume decreases. We call  $J_s(r, t)$  the fluid flux across the polymer surface such that the variation of the drop volume  $V$  writes

$$\frac{\partial V}{\partial t} = -2\pi \int_0^R J_s(r, t) r dr. \quad (12)$$

We will now find an expression for  $J_s$  using a linear poroelastic model of the substrate.

*Poroelastic model of the substrate.* The elastomer is modeled in the framework of linear poroelasticity, to solve for the chemical potential  $\mu(r, z, t)$  of the liquid. It has a constant value  $\mu_b$  within the drop and an initial value  $\mu_0$  in the polymer prior to swelling. As the drop becomes almost immediately much wider than thick ( $\theta \ll 1$ ), we can consider that the diffusion is dominated by its vertical contribution and that the radial diffusion can be neglected. That means that the radial variation of the chemical potential depends only on the initial and boundary conditions. Hence we can consider a purely 1-D diffusion of the solvent within the elastomer, allowing us to refer to previous work on one-dimensional swelling of elastomeric slabs constrained in two directions [25]. In reality, the swelling may also occur in the radial direction and this may play a role in particular when the drop radius is close to its maximal value, as fluid may diffuse away from the drop edge in the polymer, leading to an increased flux in that region. While an analytical solution for the fluid distribution was found for pinned drops [26], that solution is not valid here since we have a moving contact line. During the spreading, the drop edge moves much faster than the fluid within the polymer, while in the receding phase, the drop edge is rapidly located far away from the radial edge of the diffusion front, so that we can reasonably neglect the diffusion in the radial direction. The fluid flow in the material is thus simply driven by the vertical diffusion of the chemical potential in the elastomer:

$$\frac{\partial \mu}{\partial t} = D \frac{\partial^2 \mu}{\partial z^2}, \quad (13)$$

with initial condition  $\mu(r, z, 0) = \mu_0$  and boundary conditions  $\mu(r, 0, t) = \mu_b$  and  $\frac{\partial \mu}{\partial z} = 0$  at  $z = -H$ , with  $H$  the height of our cylinder. Technically, the upper boundary condition should be taken at  $z = u_z(r, 0, t)$  instead of  $z = 0$ , but here we can neglect the small variation in the elastomer surface position for the diffusive problem at first approximation. Utilizing the fluid incompressibility and the poroelastic stress tensor, which depends on the local concentration (and thus chemical potential), the displacement in the  $z$ -direction of the polymer can be deduced

from the following equation (see [25]):

$$\frac{\partial u_z}{\partial z} = \frac{(1 - 2\nu)(\mu - \mu_0)}{2(1 - \nu)G\Omega}, \quad (14)$$

where  $\nu$  is the poroelastic Poisson ratio,  $G$  the bulk modulus of the elastomer and  $\Omega$  the molar volume of the liquid. The poroelastic Poisson ratio defines the ability of the material to absorb fluid by swelling ( $\nu = 1/2$  corresponding to a non-swelling material). The exact value of  $\nu$  is unknown but for most elastomers,  $\nu$  is estimated to be close to 0.33 [25] which is the value we use in this study. The linearity assumption is in principle only valid for small deformations. In a complete theory, the values of  $G$  and  $D$  in particular depend on the local swelling state and could thus play a role in any elastocapillary deformations or on the overall absorption dynamics. Nevertheless, as solving the nonlinear swelling equations would require more complex simulations beyond the scope of the study, we neglect in our approach these nonlinear effects at first approximation.

For short times, when  $\sqrt{Dt} \ll H$  (which is always valid in our experiment), the potential obeys a self-similar dynamics:

$$\frac{\mu(r, z, t) - \mu_b}{\mu_0 - \mu_b} = \operatorname{erfc} \left( -\frac{z}{2\sqrt{D(t - t^*(r))}} \right), \quad (15)$$

starting for each radius  $r$  at the time  $t^*(r)$  when the elastomer is wetted by the drop. It gives the change in thickness via (14)

$$\frac{u_z(r, 0, t)}{\lambda_{max}} = 2\sqrt{\frac{D(t - t^*(r))}{\pi}}. \quad (16)$$

$\lambda_{max}$  is evaluated by comparing the size of a polymer that has swollen to its equilibrium volume when immersed in a bath of solvent in the absence of mechanical constraints to its size in the dry state, such that the volume change can be estimated as  $V_{max}/V_0 = \lambda_{max}^3$ . We can then derive (16) to find the value of  $J_s$ :

$$J_s(r, t) = \frac{\partial u_z(r, 0, t)}{\partial t} = \lambda_{max} \sqrt{\frac{D}{\pi(t - t^*(r))}}. \quad (17)$$

Combining eqs. (9), (12) and (17) we can obtain the following expression for  $v_-$ :

$$v_- = \frac{2\pi R}{3V} \int_0^R \lambda_{max} \sqrt{\frac{D}{\pi(t - t^*(r))}} r dr, \quad (18)$$

and hence the equation for the spreading dynamics:

$$\begin{aligned} \frac{dR}{dt} &= \frac{\gamma\omega}{\eta} \left( \frac{4V}{\pi R^3} + \frac{\partial u_z}{\partial r}(R, 0, t) \right)^3 \\ &\quad - \frac{2\pi R}{3V} \int_0^R \lambda_{max} \sqrt{\frac{D}{\pi(t - t^*(r))}} r dr, \end{aligned} \quad (19)$$

which we can integrate numerically. The results are presented in the next section.

**Model results.** We solve eq. (19) using an explicit Euler scheme of order 1. The values of  $D$  ( $0.45\text{--}2.34 \cdot 10^{-10} \text{ m}^2 \cdot \text{s}^{-1}$ ),  $\lambda_{max}$  (1.5),  $\gamma$  ( $18 \text{ mN} \cdot \text{m}^{-1}$ ) and  $\eta$  ( $2.3\text{--}10.5 \text{ mPa} \cdot \text{s}$ ) being known from material specifications or previous studies [23],  $\omega$  is the only fitting parameter of this model. In all that follows, its value is set to 0.05 as the best fit determined on a single experiment and is consistent with values previously reported in the literature [24]. The initial drop radius is calculated considering the drop as a half-sphere at  $t = 0$  to account for the initial spreading phase dominated by inertia [1]. Figure 6(A) shows the obtained curves for  $R(t)$  for a viscosity of  $5 \text{ mPa} \cdot \text{s}$  and different drop volumes. During the spreading phase, all the curves are almost identical, with the main differences coming later during the absorption. Qualitatively, we recover the bell-like curve obtained experimentally and the dependence of the maximal radius on the drop volume. After a fast initial increase of  $R$ , we recover the plateau-like region which is a direct consequence of the swelling. Indeed, as  $R$  increases,  $\theta$  becomes smaller and the importance of  $\theta_{tilt}$  becomes more important leading to a significant slowing down of the spreading which is also seen in the experiments. However, quantitatively, we do not retrieve the experimental values perfectly: nevertheless, our model captures the main physical ingredients of the spreading and receding of a drop, as it reproduces their main features. The model also allows us to get a good estimation of  $R_{max}$  and  $\tau_f$  (figs. 6(B), (C)). Panel (A) shows the values of  $R_{max}$  obtained numerically (dots) compared to the experimental values (crosses). We recover the fact that  $R_{max}$  depends only slightly on the oil viscosity and increases with the drop volume in a nonlinear way, which was also explained earlier. We slightly underestimate  $R_{max}$  but get a good prediction of the total absorption time. As expected, the total absorption time increases with the viscosity as well as the initial drop volume. Some other physical phenomena might also contribute to the overall dynamics. Close to the contact line, the capillary forces may deform the elastic substrate leading to viscoelastic dissipation within the material [27,28]. On very soft gels, deformations of the order of several micrometers have been reported [29,30]. In our case the typical elastocapillary length is much smaller,  $\delta = \gamma/E \simeq 20 \text{ nm}$ , so that although such elastocapillary ridge might be present and slow down the spreading, it should be small. To account for this effect, one would need to add a dissipation term coming from the solid when calculating the spreading dynamics. Furthermore, the presence of the ridge could also change the contact angle. Finally, the presence of free chains in the network, evaporation in the vicinity of the contact line, the strong approximation on the initial drop shape as well as the exact slope of the substrate close to the contact line might explain the discrepancies observed between our theory and the experiments even more. Therefore, performing more experiments, in particular on much softer elastomers would be an interesting extension of our study.

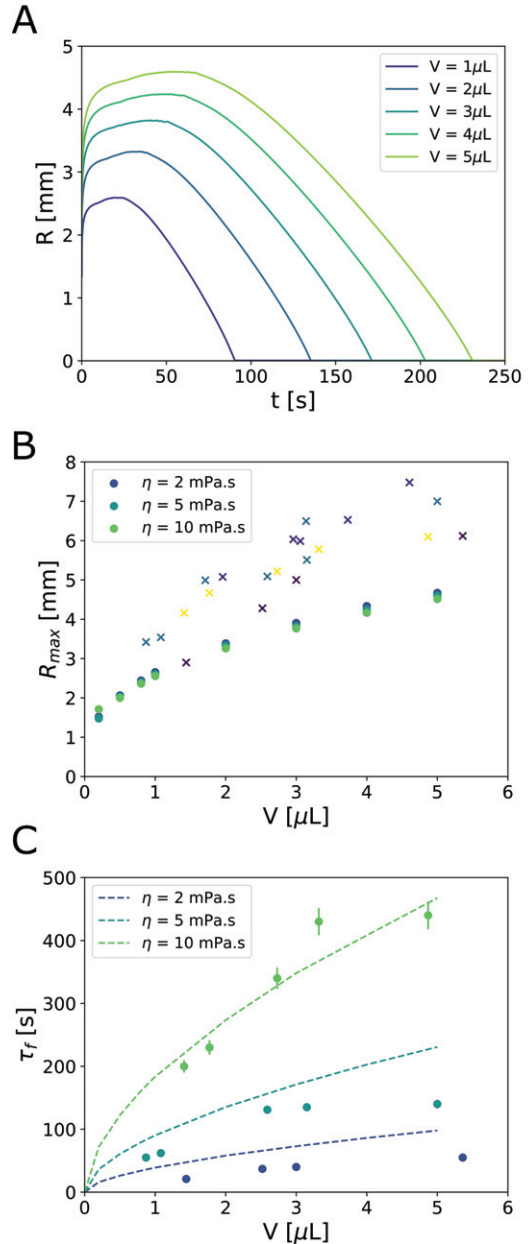


Fig. 6: Model results. (A) Model results for  $R(t)$  obtained on PVS ( $E = 0.9 \text{ MPa}$ ) with an oil viscosity of  $\eta = 5.3 \text{ mPa} \cdot \text{s}$ . (B) Obtained values of  $R_{max}$  for different oil viscosities with eq. (19) (circles) compared to the experimental data (crosses). The maximal radius depends only slightly on the oil viscosity, which is consistent with our observations. (C) Total absorption time predicted by the model (lines) *vs.* experimental values (circles).

**Discussion and conclusion.** – In this letter, we have experimentally described the absorption of a drop by a swellable flat elastomer substrate. The drop spreads quickly on the elastomer before reaching a maximal radius  $R_{max}$  and retracting as it is absorbed by the polymer. The value of  $R_{max}$  is almost independent of viscosity which can be justified by a scaling argument comparing characteristic timescales for spreading and swelling and confirmed by a

more complete model combining a Tanner-like spreading law on a tilted substrate to a linear poroelastic model of the polymer. Our model contains the main physical ingredients and can qualitatively reproduce our experimental data and predict the value of  $R_{max}$  and the total absorption time with good accuracy.

We believe the experiments and the theory presented in this paper will propose a base for further investigations of the spreading and absorption dynamics of solvent drops on absorbing and swelling substrates in different configurations.

*Data availability statement:* All data that support the findings of this study are included within the article (and any supplementary files).

## REFERENCES

- [1] BIANCE ANNE-LAURE, CLANET CHRISTOPHE and QUÉRÉ DAVID, *Phys. Rev. E*, **69** (2004) 016301.
- [2] BLAKE TERENCE D., *J. Colloid Interface Sci.*, **299** (2006) 1.
- [3] CHEBBI RACHID, *ACS Omega*, **6** (2021) 4649.
- [4] COX R. G., *J. Fluid Mech.*, **168** (1986) 169.
- [5] DE GENNES P. G., *Rev. Mod. Phys.*, **57** (1985) 827.
- [6] ESPÍN LEONARDO and KUMAR SATISH, *J. Fluid Mech.*, **784** (2015) 465.
- [7] PETROV P. and PETROV I., *Langmuir*, **8** (1992) 1762.
- [8] ROQUES-CARMES THIBAUT, MATHIEU VINCENT and GIGANTE ALEXANDRA, *J. Colloid Interface Sci.*, **344** (2010) 180.
- [9] LOHSE DETLEF, *Annu. Rev. Fluid Mech.*, **54** (2021) 349.
- [10] VAN NIEROP ERNST A., AJDARI ARMAND and STONE HOWARD A., *Phys. Fluids*, **18** (2006) 038105.
- [11] BANAHA M., DAERR A. and LIMAT L., *Eur. Phys. J. ST*, **166** (2009) 185.
- [12] ETZOLD MERLIN A., FORTUNE GEORGE T., LANDEL JULIEN R. and DALZIEL STUART B., arXiv:2202.10389 [cond-mat, physics:physics] (2022).
- [13] ZHAO MENGHUA, LEQUEUX FRANÇOIS, NARITA TETSUOHARU, ROCHÉ MATTHIEU, LIMAT LAURENT and DERRAUX JULIEN, *Soft Matter*, **14** (2018) 61.
- [14] CHATTERJEE SANGHAMITRO, MURALIDHARAN JANANI SRREE, AGRAWAL AMIT and BHARDWAJ RAJNEESH, *Phys. Fluids*, **33** (2021) 021701.
- [15] ABUKU MASARU, JANSSEN HANS, POESEN JEAN and ROELS STAF, *Build. Environment*, **44** (2009) 113.
- [16] SEVENO DAVID, LEDAUPHIN VALÉRIE, MARTIC GRÉGORY, VOUÉ MICHEL and DE CONINCK JOËL, *Langmuir*, **18** (2002) 7496.
- [17] STAROV V. M., KALININ V. V. and CHEN JING-DEN, *Adv. Colloid Interface Sci.*, **50** (1994) 187.
- [18] STAROV V. M., KOSVINTSEV S. R., SOBOLEV V. D., VELARDE M. G. and ZHDANOV S. A., *J. Colloid Interface Sci.*, **252** (2002) 397.
- [19] STAROV V. M., ZHDANOV S. A., KOSVINTSEV S. R., SOBOLEV V. D. and VELARDE M. G., *Adv. Colloid Interface Sci.*, **104** (2003) 123.
- [20] HOLMES DOUGLAS P., ROCHÉ MATTHIEU, SINHA TARUN and STONE HOWARD A., *Soft Matter*, **7** (2011) 5188.
- [21] PANDEY ANUPAM and HOLMES DOUGLAS P., *Soft Matter*, **9** (2013) 5524.
- [22] PHADNIS AKSHAY, MANNING KENNETH C., SANDERS IAN, BURGIN TIMOTHY P. and RYKACZEWSKI KONRAD, *Soft Matter*, **14** (2018) 5869.
- [23] VAN DE VELDE PIERRE, PROTIÈRE SUZIE and DUPRAT CAMILLE, *Soft Matter*, **17** (2021) 6168.
- [24] STAROV V. M., KOSVINTSEV S. R., SOBOLEV V. D., VELARDE M. G. and ZHDANOV S. A., *J. Colloid Interface Sci.*, **246** (2002) 372.
- [25] YOON JINHWAN, CAI SHENGQIANG, SUO ZHIGANG and HAYWARD RYAN C., *Soft Matter*, **6** (2010) 6004.
- [26] BOULOGNE FRANÇOIS, INGREMEAU FRANÇOIS, DERRAUX JULIEN, LIMAT LAURENT and STONE HOWARD A., *EPL*, **112** (2015) 48004.
- [27] CARRÉ ALAIN, GASTEL JEAN-CLAUDE and SHANAHAN MARTIN E. R., *Nature*, **379** (1996) 432.
- [28] LONG DIDIER, AJDARI ARMAND and LEIBLER LUDWIK, *Langmuir*, **12** (1996) 5221.
- [29] KARPITSCHKA S., DAS S., VAN GORCUM M., PERRIN H., ANDREOTTI B. and SNOELJER J. H., *Nat. Commun.*, **6** (2015) 7891.
- [30] ZHAO MENGHUA, DERRAUX JULIEN, NARITA TETSUOHARU, LEQUEUX FRANÇOIS, LIMAT LAURENT and ROCHÉ MATTHIEU, *Proc. Natl. Acad. Sci. U.S.A.*, **115** (2018) 1748.